Evolution of h/2e Aharonov-Bohm oscillation with the Zeeman energy around an antidot

Masanori Kato, Akira Endo, Shingo Katsumoto and Yasuhiro Iye

The Instutute for Solid State Physics, University of Tokyo, 5-1-5 Kashiwanoha, Kashiwa, Chiba 277-8581, Japan

Abstract

We have investigated resonant tunneling experiments through a quantum antidot in the quantum Hall regime. When the two edge states with different spins of the lowest Landau level are localized around an antidot conductance exhibits the paired $h/2e$ Aharonov-Bohm oscillations. Using a tilted magnetic field technique we observed evolution of the oscillation with the Zeeman energy. A concomitant change is observed in the conduction spectra at finite source-drain bias. These results are interpreted by the energy spacings between the single particle states with the same spin and the Zeeman splitting.

Key words: Quantum Hall effect, antidot, Aharonov-Bohm oscillation, edge channel
PACS: 73.43-f, 73.23-b

1. Introduction

A quantum antidot is a potential hill in a two-dimensional electron gas (2DEG). In the quantum Hall regime, electrons localized around an antidot form single-particle (SP) states with discrete energy levels. Tunneling probability through these states varies with a period of single flux quantum h/e per antidot area, giving rise to the Aharonov-Bohm (AB) oscillations of conductance [1,2]. In the $\nu = 2$ quantum Hall regime, where the spin-resolved edge states of the lowest Landau level (LL) are formed around the antidot, the AB oscillations with double frequency are observed [2–6]. The phenomenon reflects the energy spectrum of the antidot states, which is governed by the following two energies; the energy spacing between two successive SP states with the same spin $\Delta E_{\rm sp}$, and the Zeeman splitting $E_{\rm Z}$.

In this paper, we present a systematic study of the evolution of the AB oscillations with the Zeeman energy in the $\nu = 2$ regime. A tilted magnetic field technique has enabled us to extract the effect of Zeeman splitting on the excitation spectrum in a well-defined fashion. DC-bias spectroscopy also reveals concomitant changes. These results are compared with a simple non-interacting electron model.

2. Experiment

The device was fabricated from a GaAs/AlGaAs single heterojunction wafer with 2DEG density 3.8×10^{15} m^{-2} and mobility 60 m^2/Vs. Standard techniques of electron beam lithography, wet chemcal etching and metal evaporation were used to fabricate the device.

[1] Corresponding author. E-mail: masanori@issp.u-tokyo.ac.jp

A circular antidot of diameter 600 nm was placed in the middle of the gap between two 400 nm-wide fingers of Schottky gate, as shown in Fig. 1-(c). The separation between the antidot and each of the two gates was $\sim$ 200 nm. The two finger gates were biased independently and were used to adjust the distance between the extended edge channel(s) and the localized edge channel(s) around the antidot. Under a large negative bias, the filling factor in the constriction region $\nu_{\rm c}$ becomes less than that in the bulk of the sample $\nu_{\rm b}$. The conductance across the constriction was measured by a standard low-frequency(13 Hz) lock-in technique with a typical excitation currrent of 0.5 nA. The sample was directly immersed in the mixing chamber of a dilution refrigerator with a base temperature of $\sim$ 60 mK, and magnetic fields up to 15 T was applied. For the experimental data discussed in the next section, we fixed the bulk filling at $\nu_{\rm b} = 6$ and adjusted the gate bias to obtain $\nu_{\rm c} = 2$. In order to extract the effect of Zeeman energy $E_{\rm Z}$, the sample was tilted in-situ.

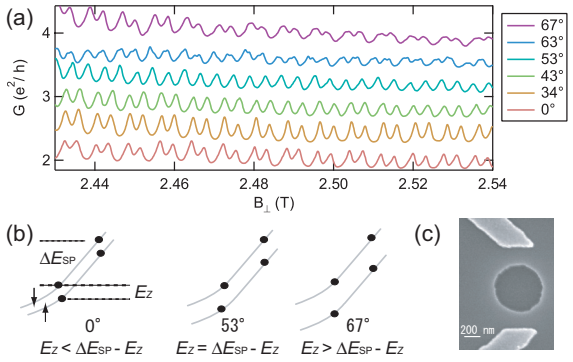

Fig. 1. (Color online) (a) Two terminal conductances G across the antidot as a function of perpendicular field component $B_{\perp}$ in the regime of $\nu_{\rm c} = 2$ on $\nu_{\rm b} = 6$ for different tilt angles θ. The successive traces are offset by $0.4e^2/h$. (b) Schematic drawings of spin-split Landau levels near the Fermi energy around the antidot with solid circles representing single-particle (SP) energy levels. While $\Delta E_{\rm sp}$ is unchanged for the same $B_{\perp}$, $E_{\rm Z}$ which is proportional to the total B increases. (c) Scanning electron microscope (SEM) image of the device.

3. Results and Discussion

Figure 1-(a) shows the two-terminal conductances G through the constriction under the condition of $\nu_{\rm b} = 6$ and $\nu_{\rm c} = 2$ as a function of the perpendicular field component $B_{\perp}$. In this situation, two channels of spin-split lowest Landau levels (LLs) encircle the antidot while the higher LL edge channels are reflected by the constriction. The lowermost trace for $\theta = 0^{\circ}$ exhibits AB oscillations that occur as a series of double-peaks rising above the approximately constant baseline at $\sim 2e^2/h$. These peaks are manifestation of partial transmission of second lowest LL edge channels via tunneling into (and out of) the lowest LL edge channels localized around the antidot. The double-peak structure is naturally attributed to inter-LL tunneling between spin-resolved edge channels. Figure 1-(a) shows evolution of the double-peaked AB oscillation as the sample is tilted. It is seen that the spacing between the twin peaks increases with increasing θ. The peaks becomes almost equally spaced at $\theta = 53^{\circ}$. Further increase of θ restores the double-peak structure.

This behavior can be understood by considering the spin-resolved single-particle spectrum such as illustrated in Fig. 1-(b).[3,4] With increasing θ, the Zeeman energy $E_{\rm Z}$ becomes larger for the same $B_{\perp}$. The energy spacing between antidot states with an opposite spin alternates between $E_{\rm Z}$ and $\Delta E_{\rm sp} - E_{\rm Z}$. At $\theta = 0^{\circ}$, $E_{\rm Z}$ is smaller than $\Delta E_{\rm sp}/2$. As θ is increased, $E_{\rm Z}$ increases and coincides with $\Delta E_{\rm sp}/2$ at $\theta \simeq 53^{\circ}$. When θ is increased further, $E_{\rm Z}$ becomes larger than $\Delta E_{sp} - E_{\rm Z}$ and the pair structure emerges again.

In order to verify the validity of the above picture we have investigated the dependence of the conductance on the source-drain bias $V_{\rm SD}$. Figure 2-(a) is a grey-scale plot of the conductance on the $(B_{\perp}, V_{\rm SD})$ plane for $\theta = 0^{\circ}$ and 53° showing halves of diamond patterns. Finite $V_{\rm SD}$ causes splitting of individual peaks. Each of the split pair corresponds to the coincidence of a particular SP state with the electrochemical potential of either the source or the drain lead. Adjacent peaks cross when the applied bias equals the energy difference between the two states plus the charging energy e^2/C. Therefore the apices of the larger diamonds give $\Delta E_{\rm sp} - E_{\rm Z} + e^2/C$ while those of the smaller diamonds give $E_{\rm Z} + e^2/C$ at $\theta = 0^{\circ}$ as shown in the previous works [5,6]. At $\theta = 53^{\circ}$ the diamonds becomes nearly uniform in size. In Fig. 2-(b), the energy spacings obtained from the diamonds for the several tilt angles in Fig. 1-(a) show systematic changes with the total magnetic field, that is with the Zeeman energy $E_{\rm Z}$. The dashed straight lines in Fig. 2-(b) represent

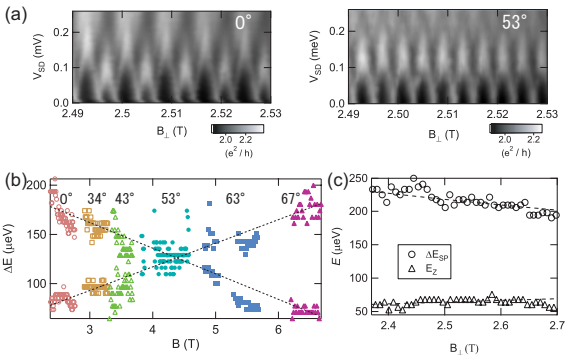

Fig. 2. (Color online) (a) Grey-scale plots of the differential conductance as a function of $B_\perp$ and $V_{\rm SD}$ under the condition of $\nu_{\rm b} = 6$ and $\nu_{\rm c} = 2$. The two figures are for the tilt angle $\theta = 0°$ (left) and 53° (right), respectively. (b) Evolution of the energy splitting ΔE with the total field B. Different symbols represent the energy spacing obtained from the DC-bias measurement at different tilt angles. The dashed straight lines represent B-linear fit. (c) Dependence of the energy gaps on the perpendicular magnetic field. Circles and triangles represent $\Delta E_{\rm sp}$ and $E_{\rm Z}$, respectively. These data are obtained from the data of $\theta = 0°$ in (b). The dashed curve drawn through the $\Delta E_{\rm sp}$ data represents the $1/B$ dependence, while the dotted line drawn through the $E_{\rm Z}$ data represents the B-linear dependence.

$\Delta E_{\rm sp} - E_{\rm Z} + e^2/C$ (down-slope line) and $E_{\rm Z} + e^2/C$ (up-slope line), respectively. From these lines, the g-factor is evaluated as $g \sim 0.4$ and the charging energy $e^2/C \simeq 21$ μeV.

Once we determine the charging energy and assume that it stays constant over the field range of interest, we can extract the values of $\Delta E_{\rm sp}$ and $E_{\rm Z}$ directly from the experimental values of ΔE in Fig. 2-(b). The $B_\perp$-dependence of $\Delta E_{\rm sp}$ and $E_{\rm Z}$ thus extracted are plotted in Fig. 2-(c) for $\theta = 0°$. From the B-linear dependence of $E_{\rm Z}$, the g-factor is determined as $|g| = 0.44$, which is essentially the same as that of bulk GaAs.

The energy separation $\Delta E_{\rm sp}$ of SP states around a circular antidot of radius r can be expressed as $\Delta E = h/(2\pi r B_\perp)|{\rm d}V/{\rm d}r|$, where ${\rm d}V/{\rm d}r$ is the slope of the antidot potential. The antidot potential $V(r)$ includes the effect of screening[7] and can generally be $B_\perp$-dependent. If that dependence is weak enough, $\Delta E_{\rm sp} \propto 1/B_\perp$. The dashed curve drawn through the $\Delta E_{\rm sp}$ data in Fig. 2-(c) represents a $1/B_\perp$-dependence. The good fit to the $1/B_\perp$-dependence indicates that the screening effect is rather weak, which is consistent with the small value of the charging energy as compared to $\Delta E_{\rm sp}$ in this case.

We have seen that the experimental results under $\nu_{\rm b} = 6$ and $\nu_{\rm c} = 2$ can be interpreted in terms of a nearly-noninteracting electron picture. When the bulk filling was set $\nu_{\rm b} = 4$, similar analysis yielded a much larger charging energy, $e^2/C \simeq 60$ μeV, and the $B_\perp$-dependence of $\Delta E_{\rm sp}$ shows some deviation from the simple picture. When the bulk filling was set $\nu_{\rm b} = 3$, the AB oscillations ceased to show such a clear evolution with θ as the case of $\nu_{\rm b} = 6$. These results imply that at higher magnetic field such a simple noninteracting picture like the one depicted in Fig. 1-(b) is no longer valid, as pointed out by Michael et al.[6]

4. Conclusion

We have systematically extracted the effect of Zeeman energy on the evolution of the $h/2e$ AB oscillations at $\nu_{\rm c} = 2$ from the tilted-field experiments. The evolution of the double-peak structure and the concomitant changes in the conduction spectra as a function of $V_{\rm SD}$ and $B_\perp$ are observed. For sufficiently high bulk filling ($\nu_{\rm b} = 6$), the results are consistently interpreted within the simple picture of spin-resolved single-particle states with Zeeman splitting.

The work is supported in part by Grant-in-Aid for Scientific Research and by Special Coordination Funds for Promoting Science and Technology and from the Ministry of Education, Culture, Sports, Science and Technology (MEXT) Japan.

References

[1] V.J. Goldman and B. Su, Science 267 (1995) 1010.

[2] C.J.B. Ford et al., Phys. Rev. B 49 (1994) 17456.

[3] D.R. Mace et al., Phys. Rev. B 52 (1995) R8672.

[4] M. Kataoka et al., Physica E 12 (2002) 782.

[5] M. Kataoka et al., Phys. Rev. Lett. 83 (1999) 160.

[6] C.P. Michael et al., Physica E 34 (2006) 195.

[7] I. Karakurt et al., Phys. Rev. Lett. 87 (2001) 146801-1.